

Supplement of

Implementing the Nitrogen cycle into the dynamic global vegetation, hydrology and crop growth model LPJmL

W. von Bloh et al.

Correspondence to: Werner von Bloh (bloh@pik-potsdam.de)

S1 Supplementary information to the nitrogen implementation of the LPJmL 5 model

The supplement contains a table of parameters used in the model (Table S1) and graphical representations of leaf C:N ratios for different exponential factors (Fig. S1), daily gross photosynthesis rate as a function of light- and Rubisco limited photosynthesis rate (Fig. S2), temperature response function $F_1(T)$ (Fig. S3), and water response function $F_2(W)$ (Fig. S4). Furthermore 5 comparisons of net ecosystem exchange rates and evaporation fluxes with EDDY flux tower measurements (ORNL DAAC, 2011) for a variety of sites are shown (Figs. S5-S11 and Figs. S12-S20, respectively). Wheat, rice and soybean simulations for the 10 top-producing countries for the carbon-only LPJmL 3.5 version, the version with N limitation and with unlimited N supply are shown in Figs. S21-S23.

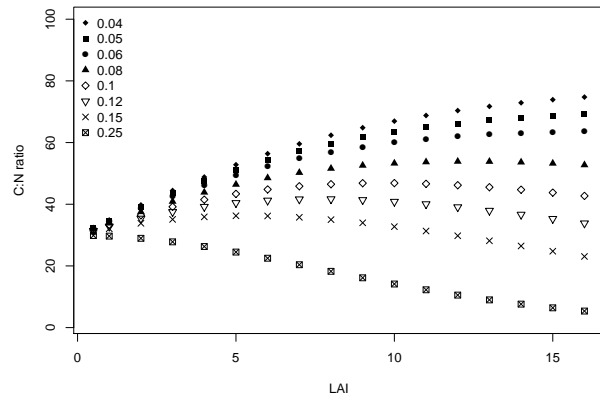


Figure S1. Leaf C:N ratio of the canopy as a function of LAI for different pre-factors of the exponential term in Eq. (2).

Parameter	Description	Value	Units
θ	Shape parameter for co-limitation of photosynthesis	0.9	-
$N_{\text{up,root}}$	Maximum N uptake rate	2.8 (trees), 5.51 (grass and crops)	gN KgC^{-1}
$K_{\text{N,min}}$	Michaelis constant of N uptake	1.48	gN m^{-2}
$k_{\text{N,min}}$	Basal rate of N uptake	0.05	-
k_{store}	Increase in N demand	1.15 (trees), 1.3 (grass and crops)	-
k_{turn}	N recover fraction at turnover	80 (evergreen PFTs), 30 (other PFTs)	%
$f_{\text{heartwood}}$	Fraction of sapwood nitrogen going into heartwood	0.7	-
K_M	Michaelis constant of photosynthesis reduction	0.1	-
K_{max}	Maximum rate of NH_4^+ nitrified	0.1	d^{-1}
a	Parameter in limiting function for temperature $F_1(T)$	8.79	$^{\circ}\text{C}$
b	Parameter in limiting function for temperature $F_1(T)$	5.26	-
a_{nit}	Parameter in water response function $F_1(W_{\text{sat}})$	0.6 (medium soil), 0.55 (sandy soil)	-
b_{nit}	Parameter in water response function $F_1(W_{\text{sat}})$	1.27 (medium soil), 1.7 (sandy soil)	-
c_{nit}	Parameter in water response function $F_1(W_{\text{sat}})$	0.001 (medium soil), -0.007 (sandy soil)	-
d_{nit}	Parameter in water response function $F_1(W_{\text{sat}})$	2.84 (medium soil), 3.22 (sandy soil)	-
CDN	Shape coefficient for $F_2(T, C)$	1.4	-
A_f	Fraction of decomposed N mineralized	0.7	-
F_f	Fraction of humified N going into fast pool	0.98	-
$\beta_{\text{NO}_3^-}$	NO_3^- percolation coefficient	0.4	-
CN _{soil}	Desired C:N ratio of soils	15	-
k_{soil10}^f	Decomposition rate of fast pool	0.03	yr^{-1}
k_{soil10}^s	Decomposition rate of slow pool	0.001	yr^{-1}
k_{nit}	Fraction of mineralized N nitrified to NO_3^-	0.2	-
r_{mx}	Fraction of denitrified N lost as N_2O	0.11	-
θ	Fractional pore space	0.4	-
K_2	Fraction of nitrified N lost as N_2O flux	0.02	-
K_N	Michaelis constant of N immobilization	5×10^{-3}	gN m^{-3}
T_0	Parameter in temperature uptake function	-25	$^{\circ}\text{C}$
T_m	Parameter in temperature uptake function	15	$^{\circ}\text{C}$
T_r	Parameter in temperature uptake function	15	$^{\circ}\text{C}$
q_{ash}	Fraction of fire N going to the top soil layer	0.45	-

Table S1. List of parameters used in the LPJmL 5 model.

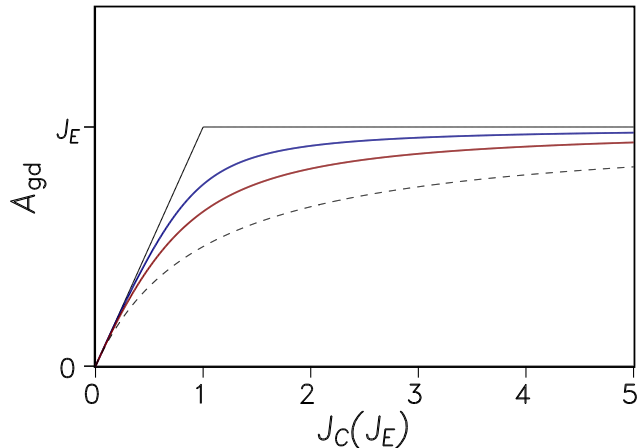


Figure S2. Daily gross photosynthesis rate A_{gd} as a function of Rubisco-limited photosynthesis rate J_C for fixed light-limited rate J_E and daylength set to 1. The black solid curve is for shape parameter $\theta = 1$ ($A_{\text{gd}} = \min(J_E, J_C)/\text{daylength}$), the blue curve for $\theta = 0.9$ (LPJmL 5), the red curve for $\theta = 0.7$ (LPJmL 3.5) and the black dashed curve for $\theta \rightarrow 0$ ($A_{\text{gd}} = J_E \cdot J_C / ((J_E + J_C) \cdot \text{daylength})$).

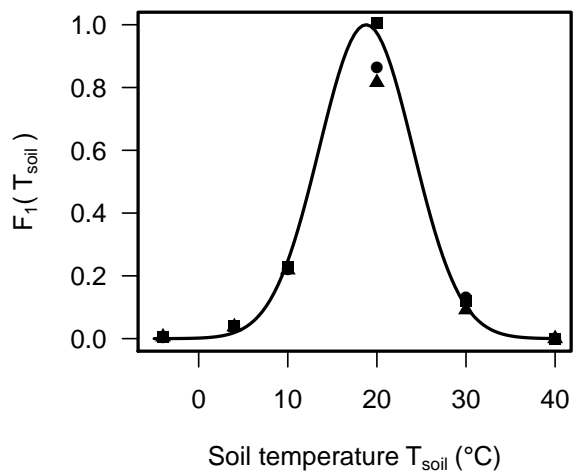


Figure S3. Temperature response data for site in the US (filled squares), Canada (filled circles) and Australia (filled triangles) and fitted function (solid line).

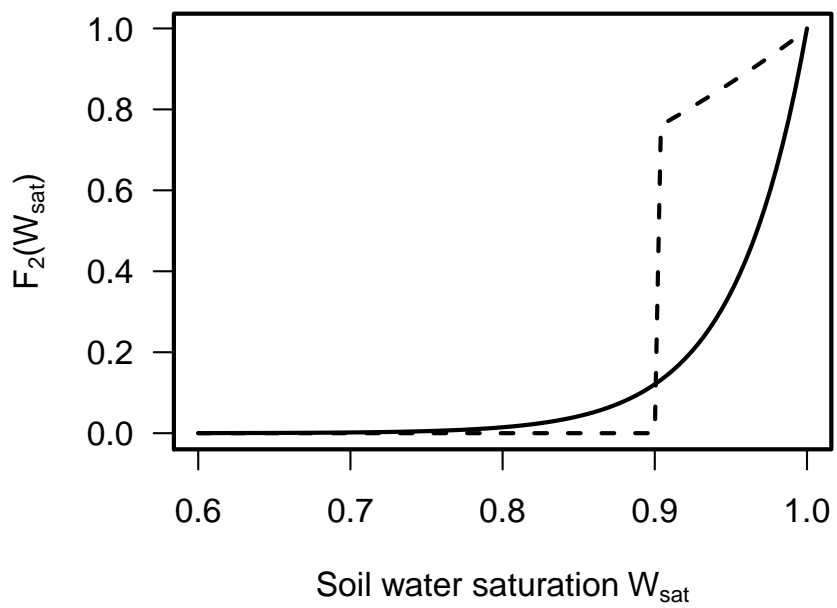


Figure S4. Water response functions $F_2(W_{\text{sat}})$ parameterized according to Krysanova and Wechsung (2000) (dashed line) and according to Eq. (43) in the main text (solid line).

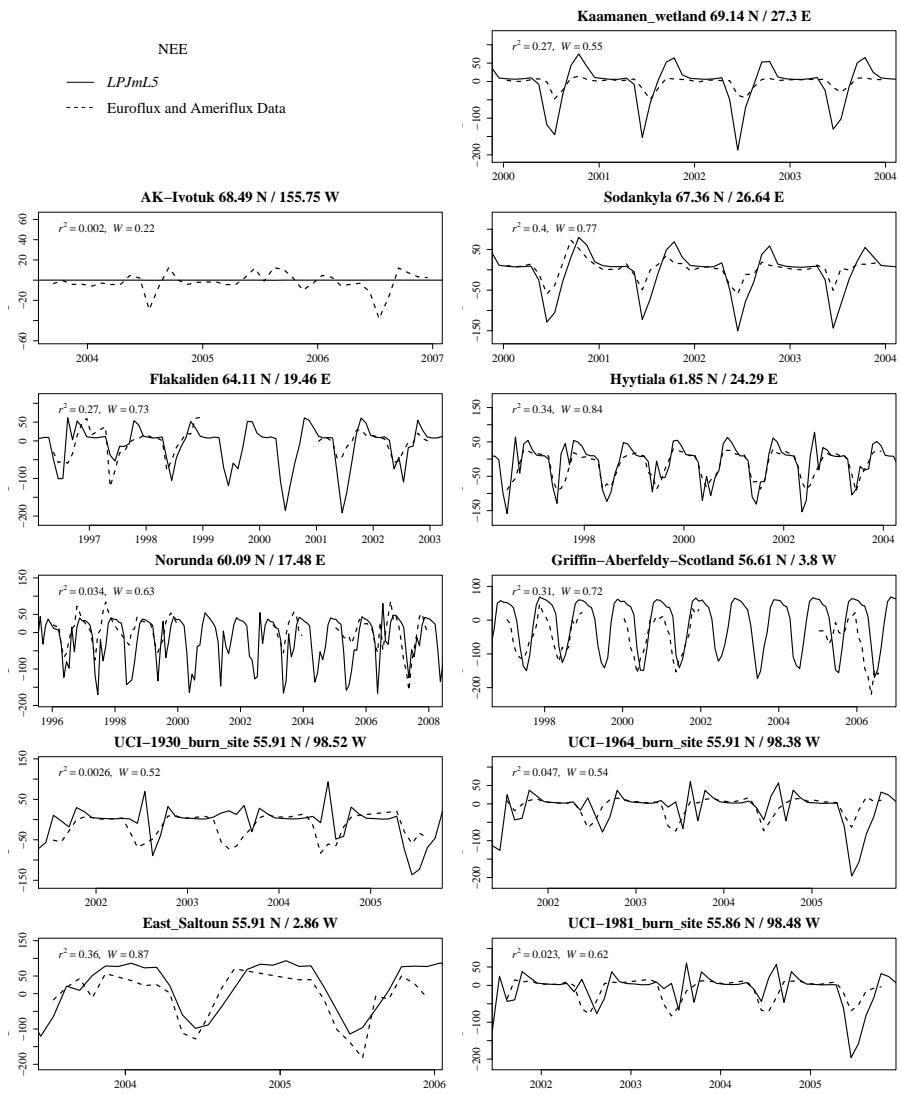


Figure S5. Comparison of net ecosystem exchange rates (NEE, in $\text{gC m}^{-2} \text{d}^{-1}$) simulated with eddy flux tower rates measured.

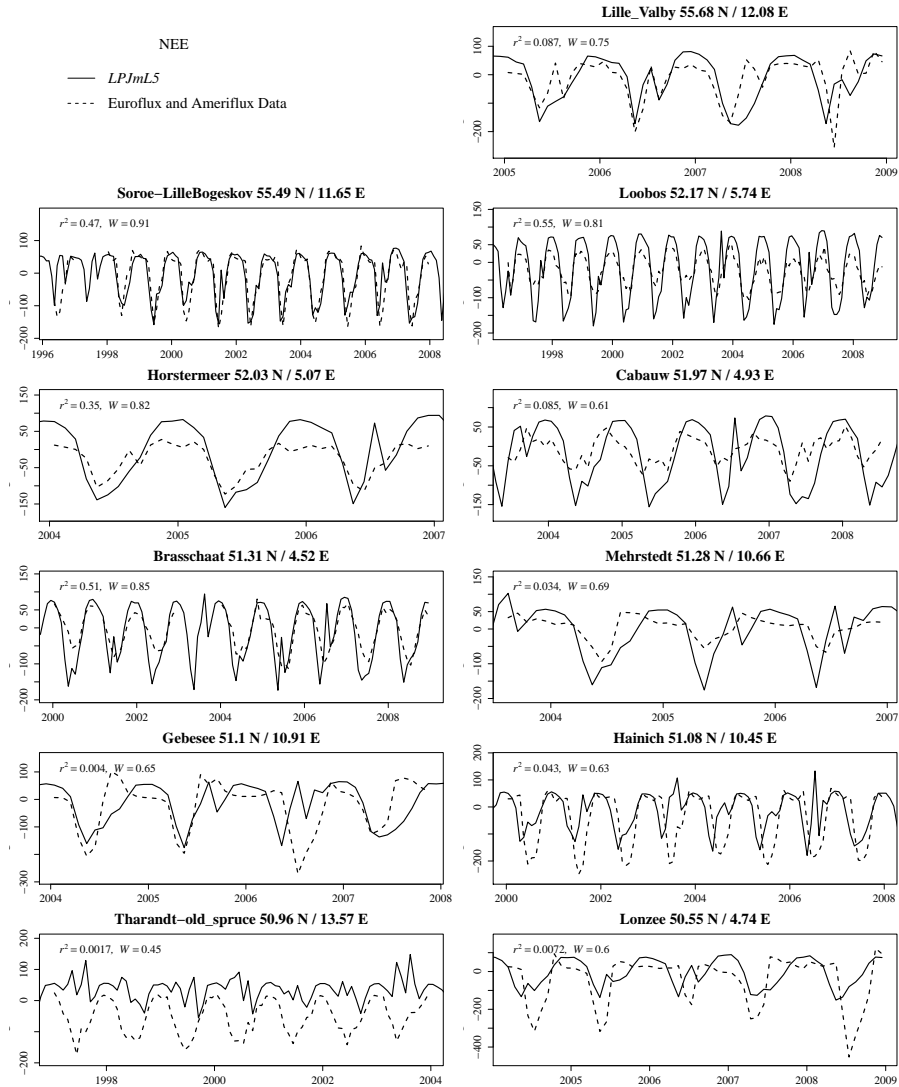


Figure S6. Comparison of net ecosystem exchange rates (NEE, in $\text{gC m}^{-2} \text{d}^{-1}$) simulated with eddy flux tower rates measured.

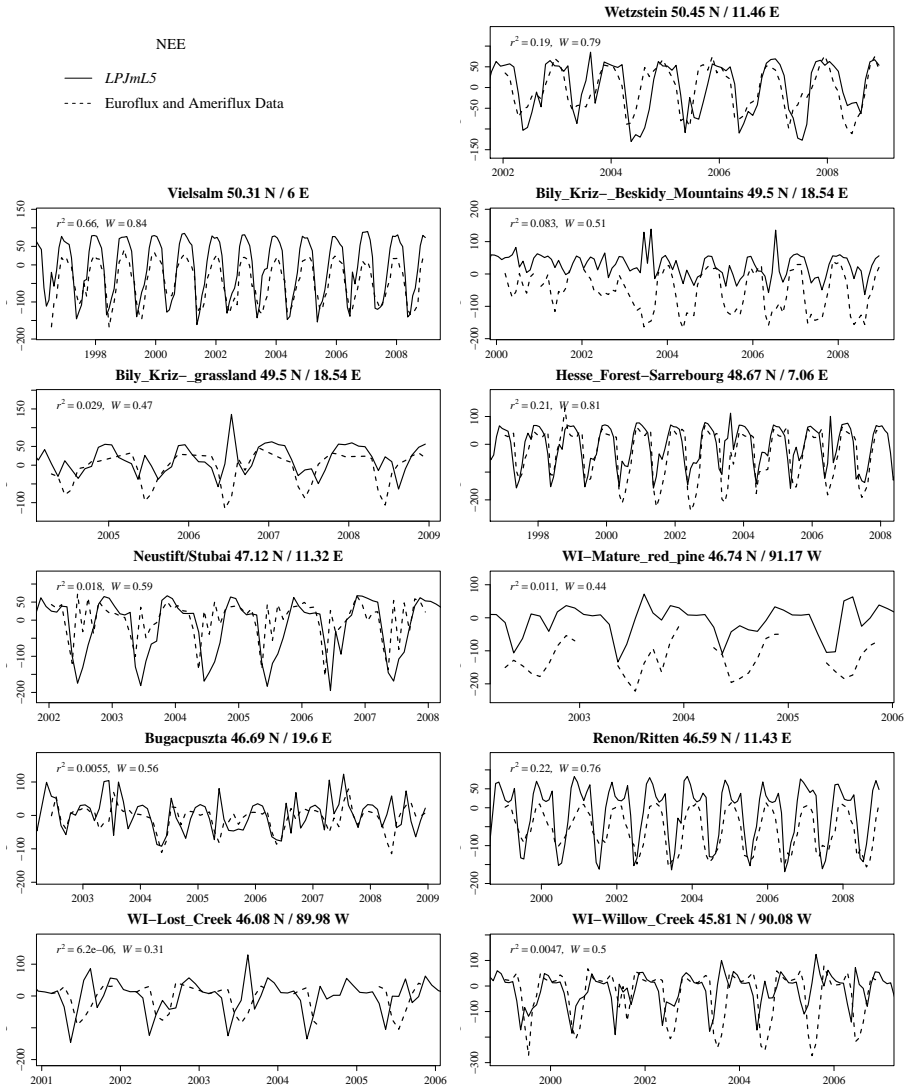


Figure S7. Comparison of net ecosystem exchange rates (NEE, in $\text{g C m}^{-2} \text{ d}^{-1}$) simulated with eddy flux tower rates measured.

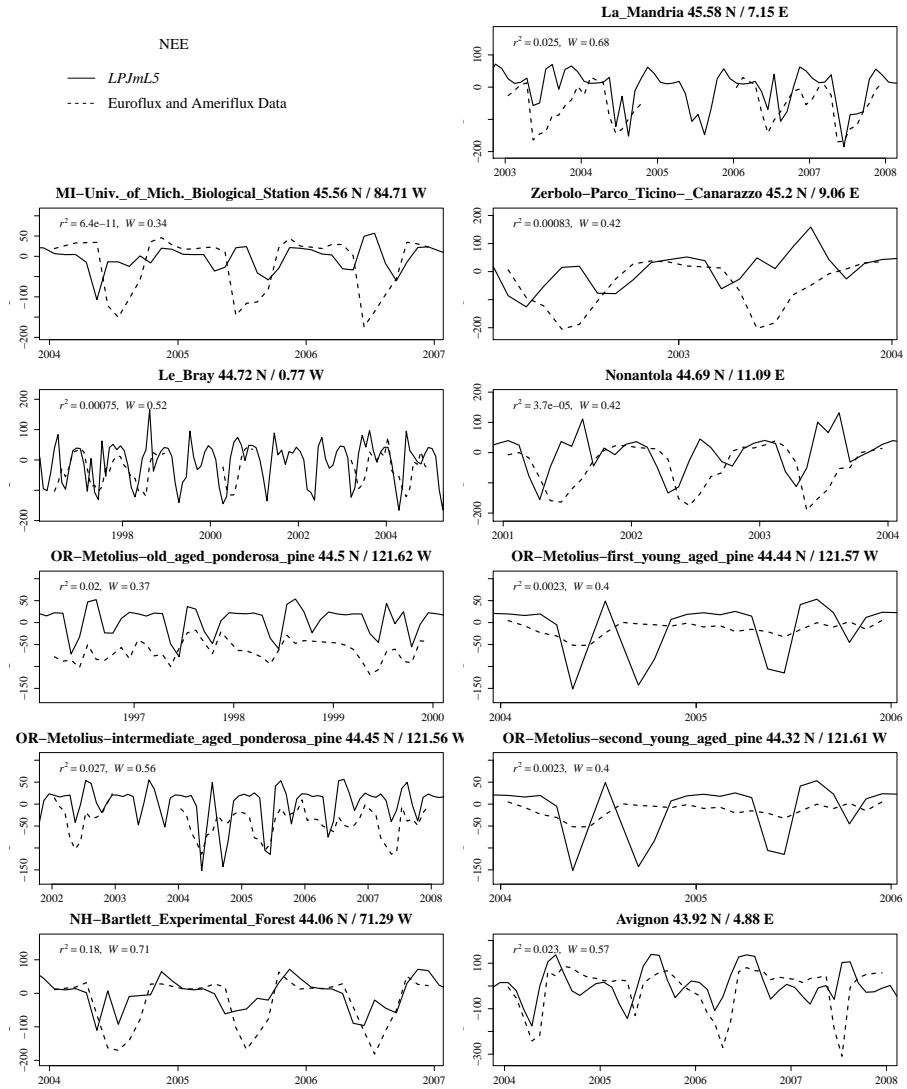


Figure S8. Comparison of net ecosystem exchange rates (NEE, in $\text{gC m}^{-2} \text{d}^{-1}$) simulated with eddy flux tower rates measured.

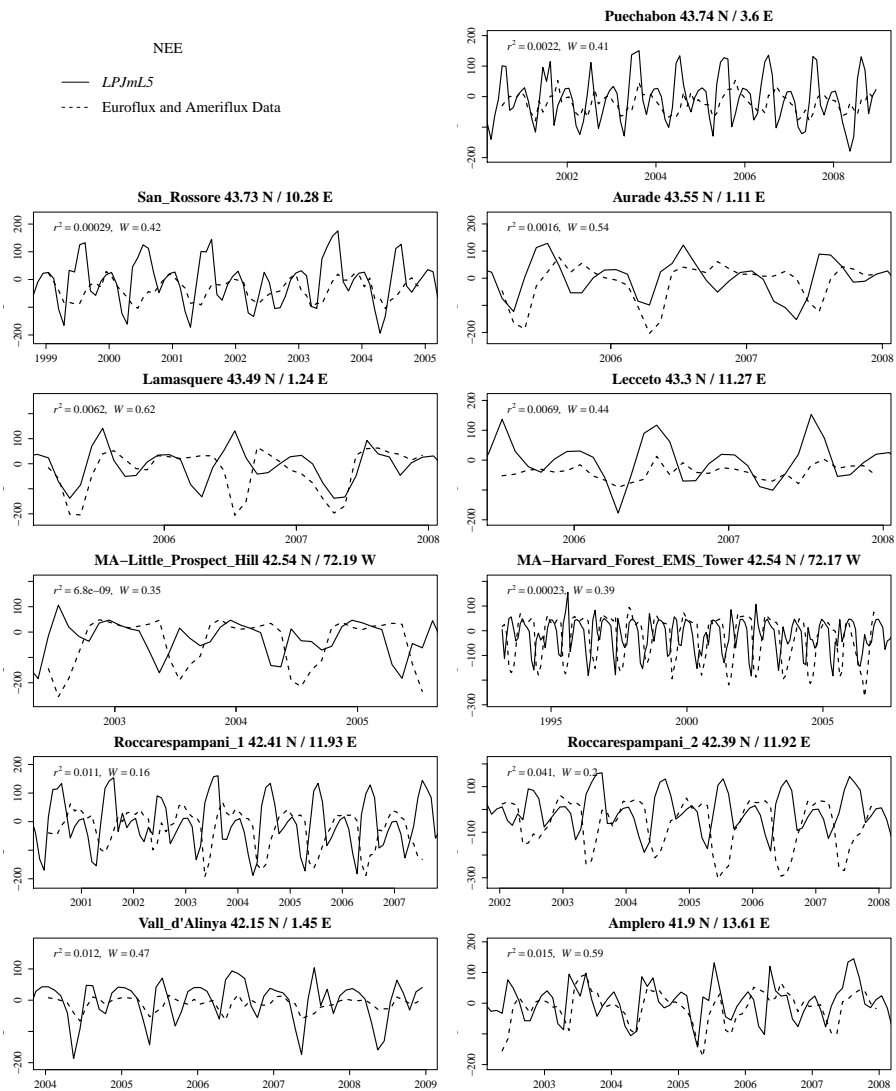


Figure S9. Comparison of net ecosystem exchange rates (NEE, in $\text{gC m}^{-2} \text{ d}^{-1}$) simulated with eddy flux tower rates measured.

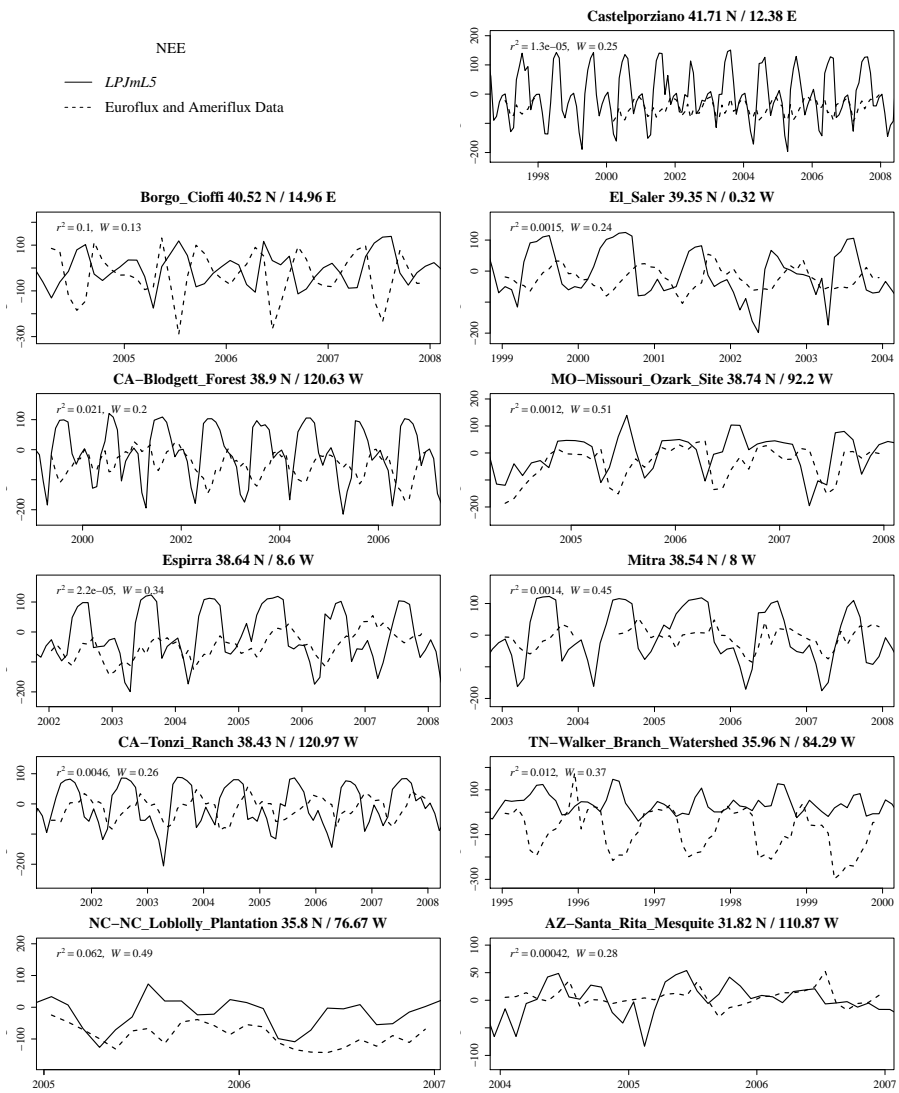


Figure S10. Comparison of net ecosystem exchange rates (NEE, in $\text{gC m}^{-2} \text{ d}^{-1}$) simulated with eddy flux tower rates measured.

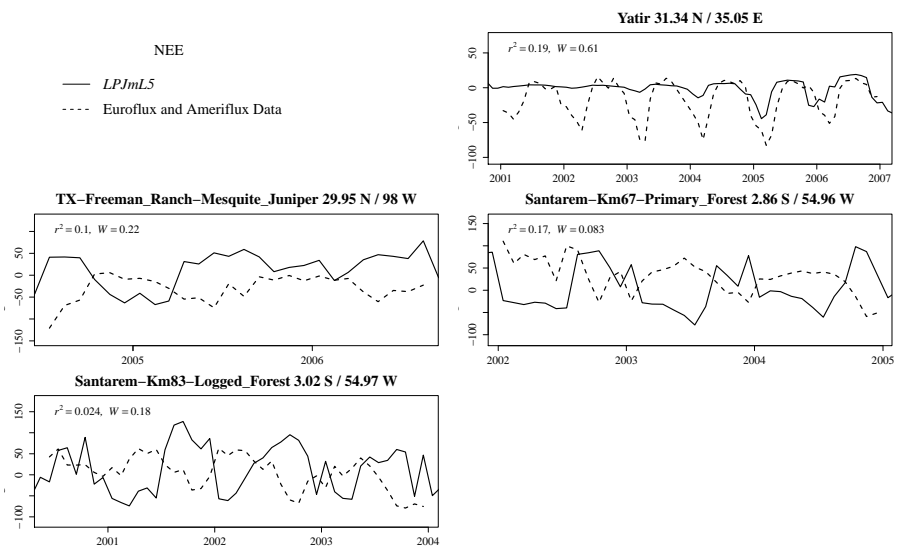


Figure S11. Comparison of net ecosystem exchange rates (NEE, in $\text{gC m}^{-2} \text{ d}^{-1}$) simulated with eddy flux tower rates measured.

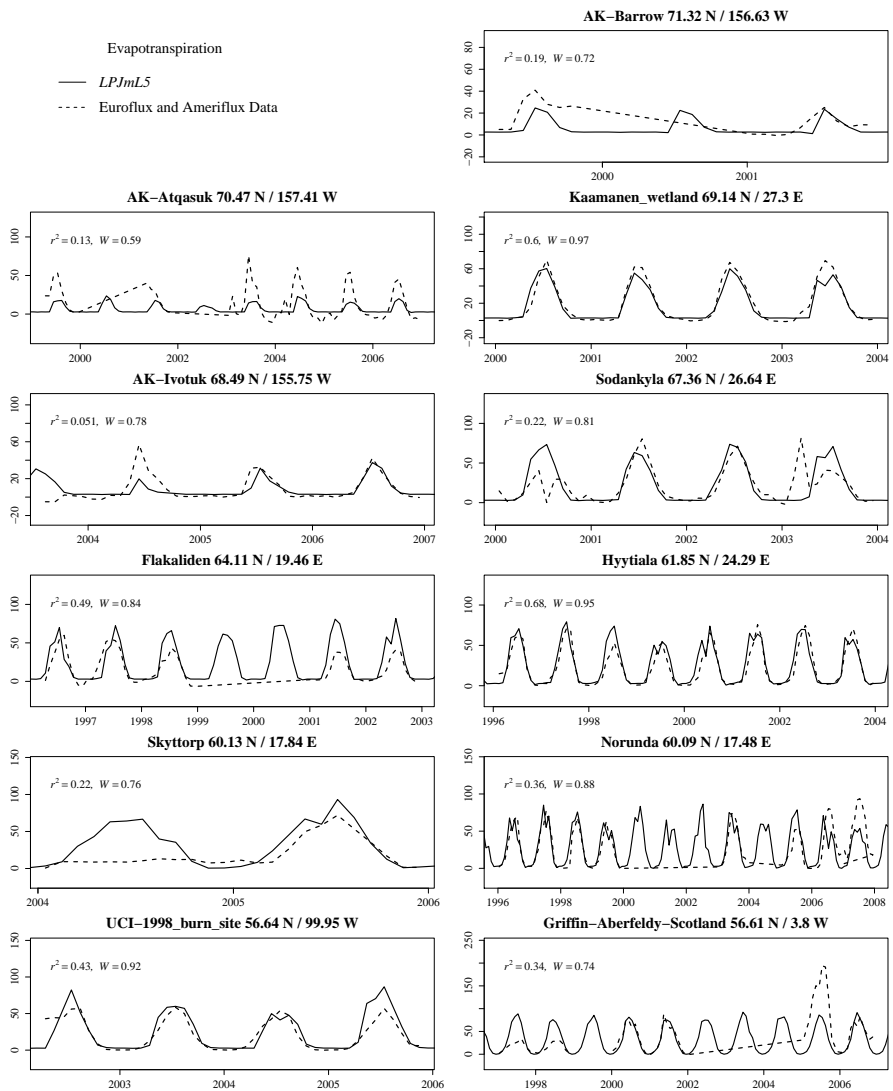


Figure S12. Comparison of evapotranspiration fluxes (in mm d^{-1}) with EDDY-flux measurements.

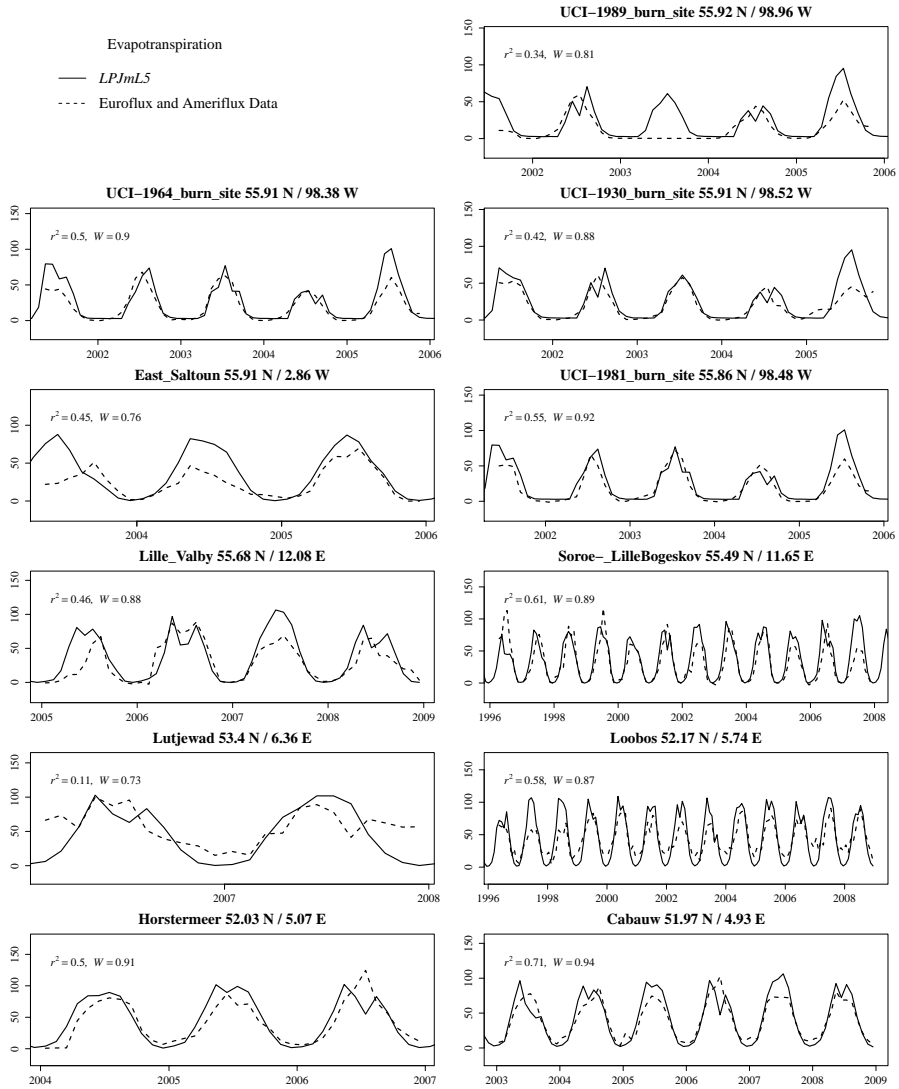


Figure S13. Comparison of evapotranspiration fluxes (in mm d^{-1}) with EDDY-flux measurements.

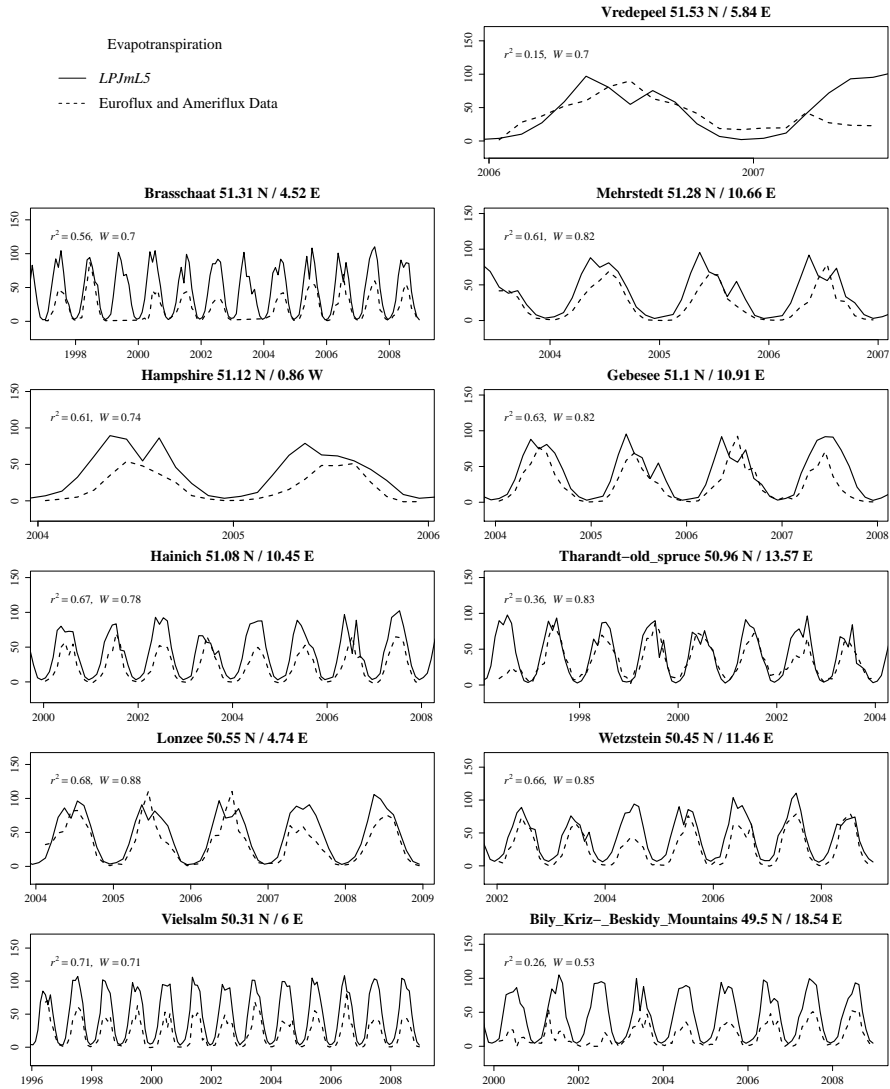


Figure S14. Comparison of evapotranspiration fluxes (in mm d^{-1}) with EDDY-flux measurements.

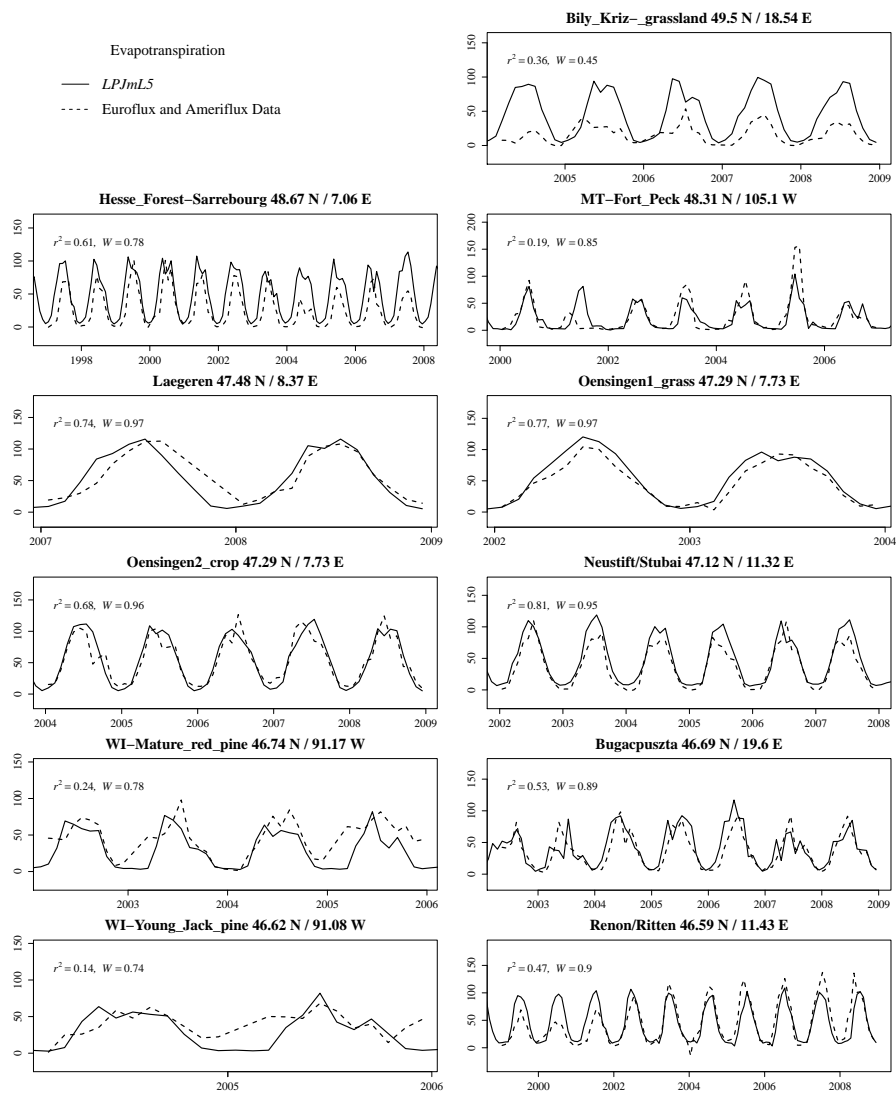


Figure S15. Comparison of evapotranspiration fluxes (in mm d^{-1}) with EDDY-flux measurements.

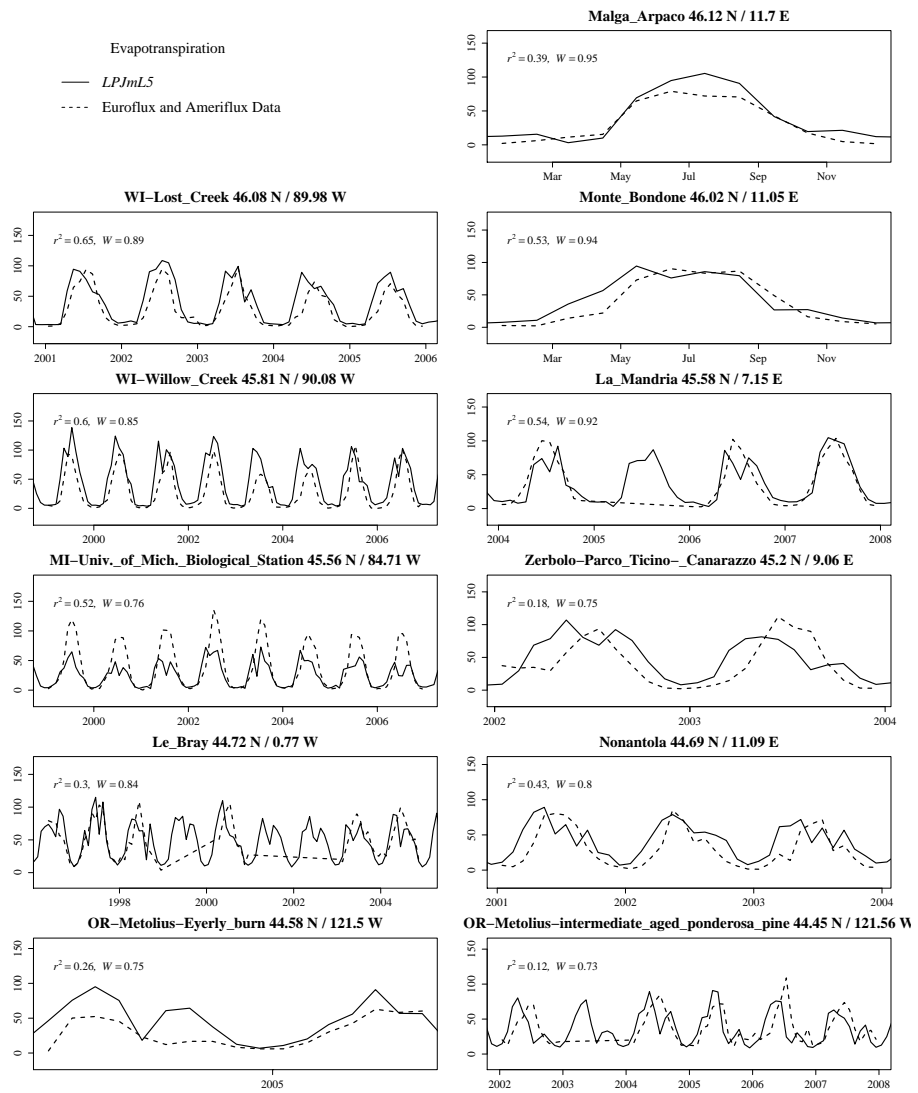


Figure S16. Comparison of evapotranspiration fluxes (in mm d^{-1}) with EDDY-flux measurements.

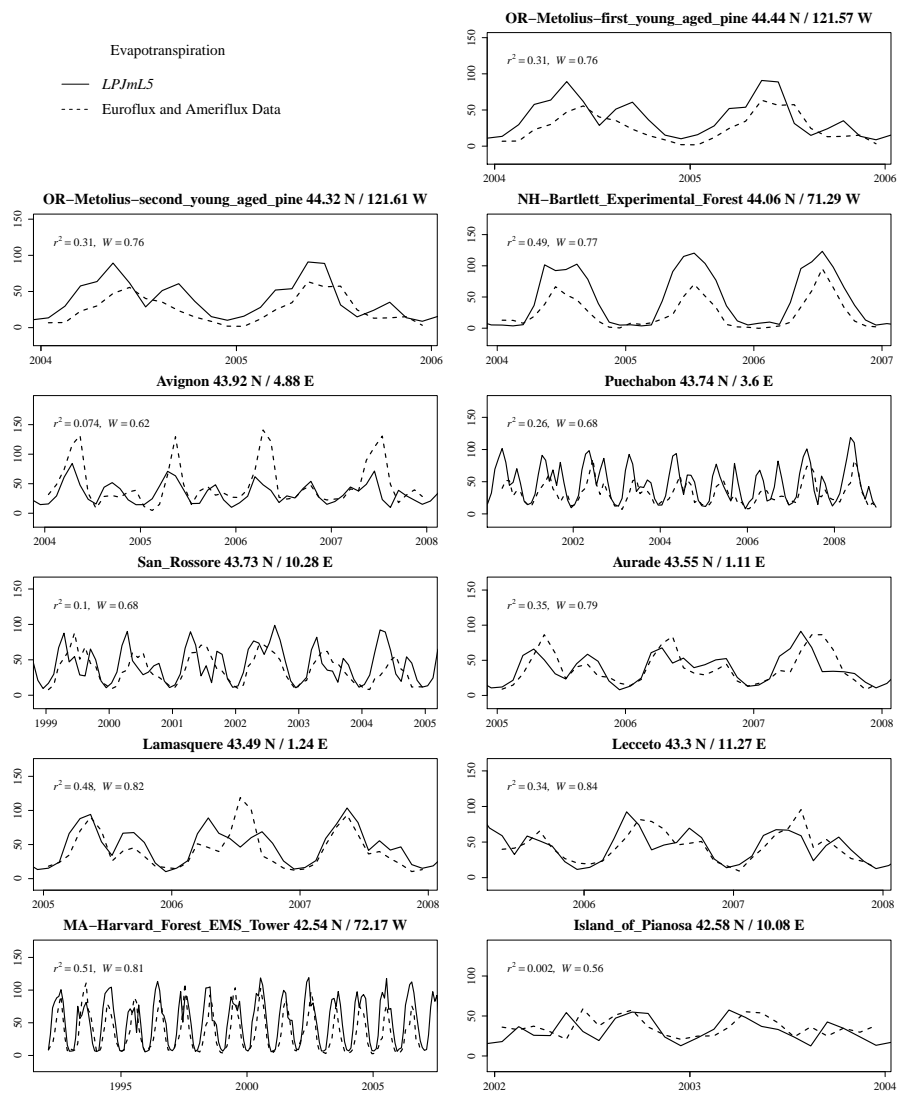


Figure S17. Comparison of evapotranspiration fluxes (in mm d^{-1}) with EDDY-flux measurements.

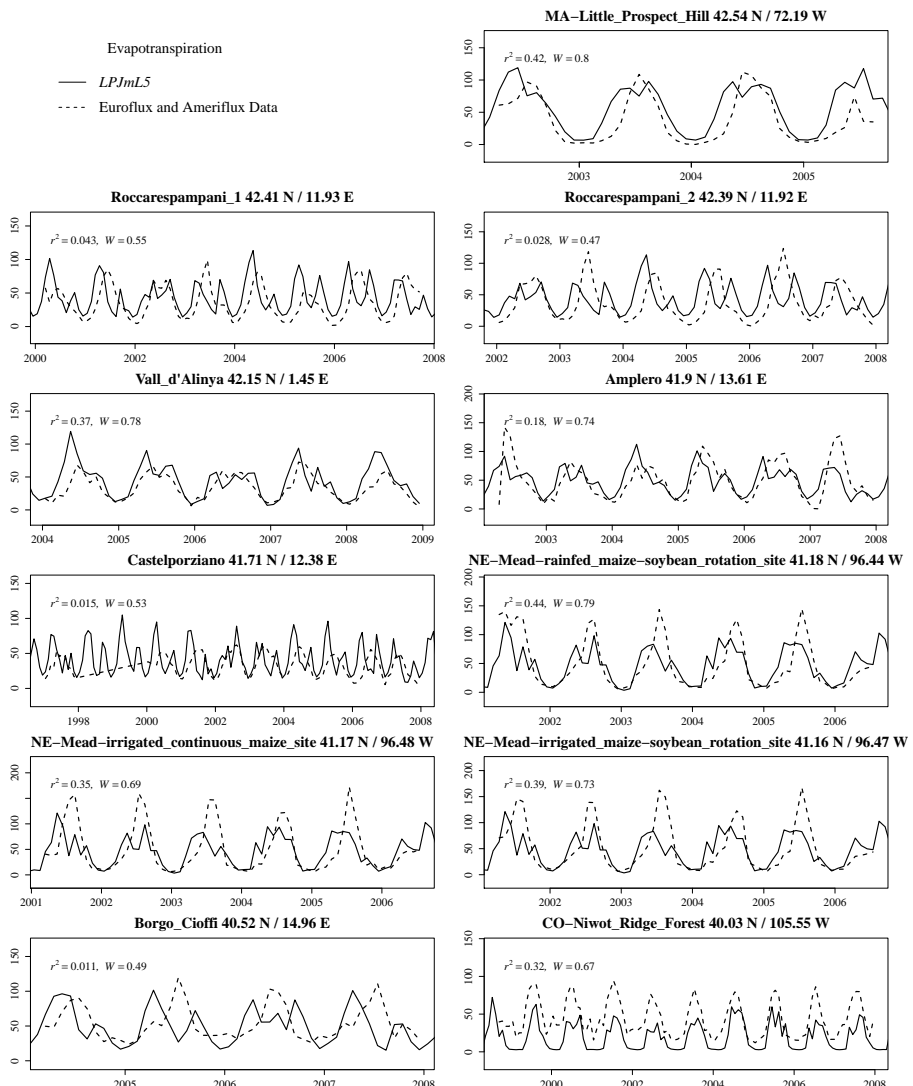


Figure S18. Comparison of evapotranspiration fluxes (in mm d^{-1}) with EDDY-flux measurements.

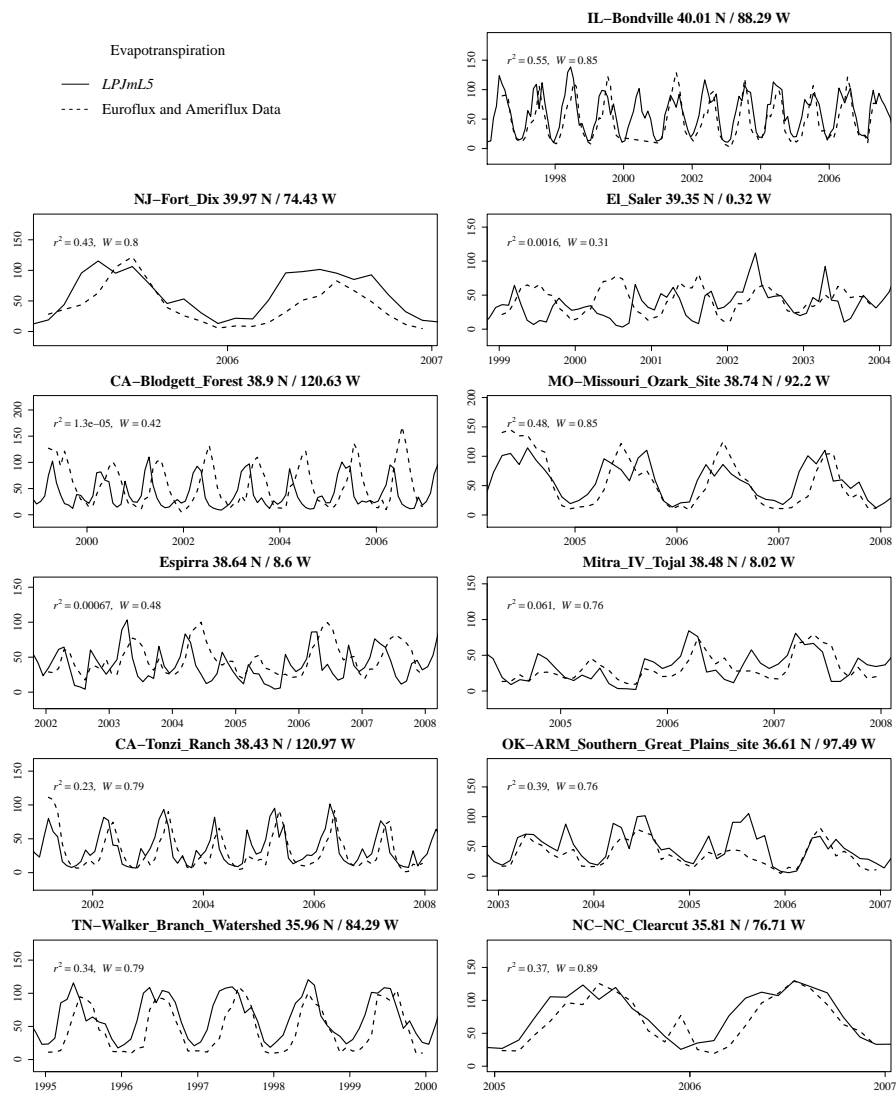


Figure S19. Comparison of evapotranspiration fluxes (in mm d^{-1}) with EDDY-flux measurements.

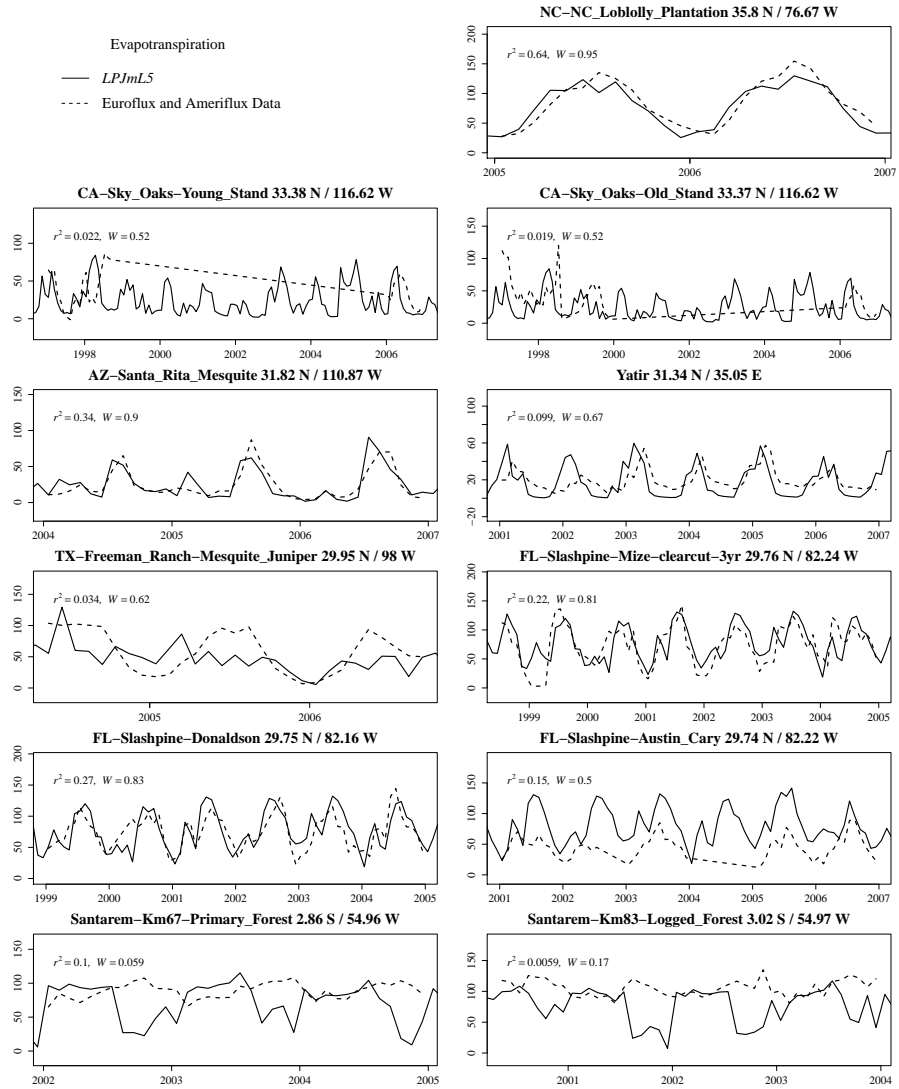


Figure S20. Comparison of evapotranspiration fluxes (in mm d^{-1}) with EDDY-flux measurements.

References

- Krysanova, V. and Wechsung, F.: SWIM (Soil and Water Integrated Model) User Manual, <https://www.pik-potsdam.de/members/valen/swim>,
2000.
- ORNL DAAC, Oak Ridge, T. U.: Oak Ridge National Laboratory Distributed Active Archive Center (ORNL DAAC), <http://fluxnet.ornl.gov/>,
5 2011.

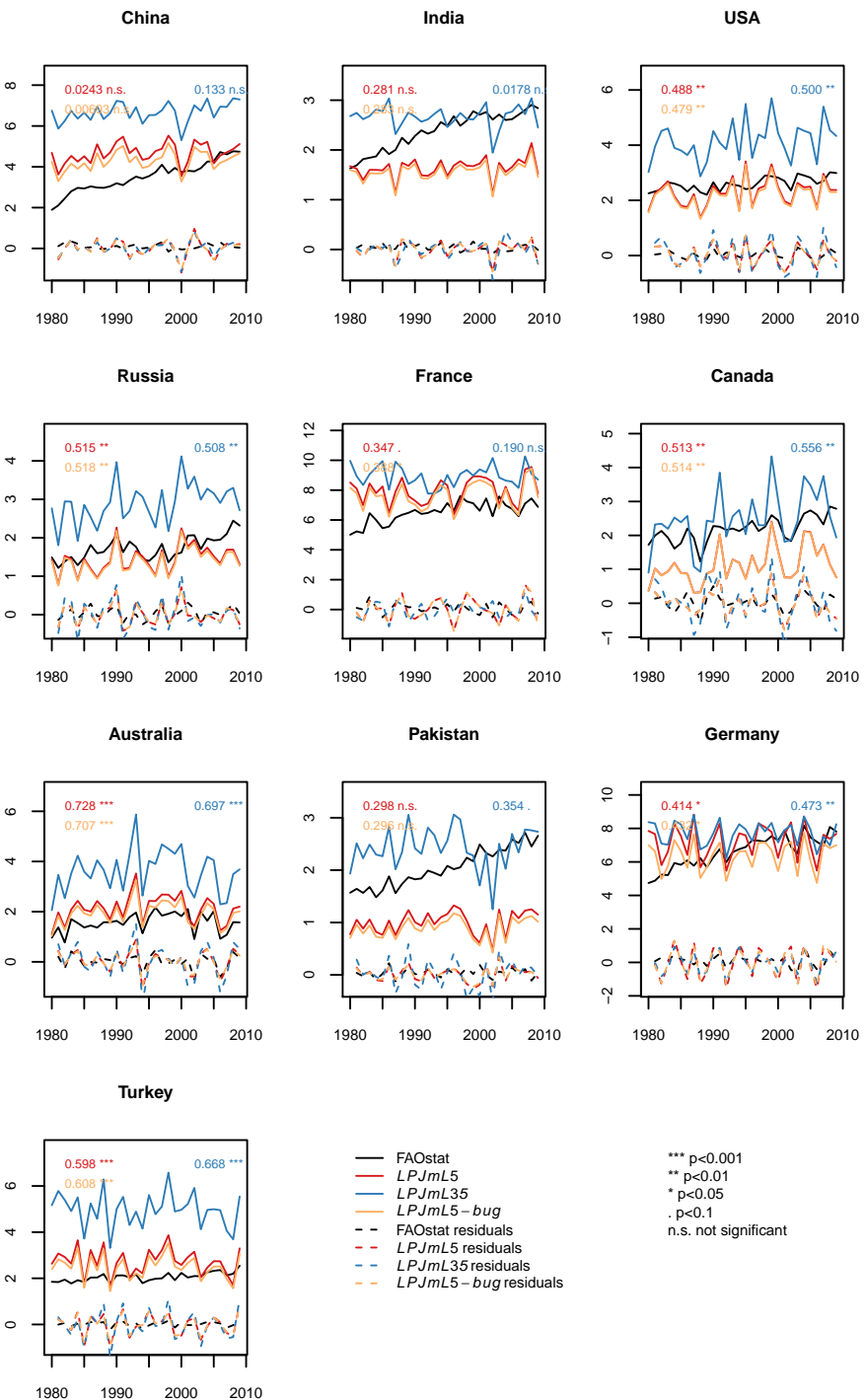


Figure S21. Wheat yield simulations (in tFM ha⁻¹) for the 10 top-producing countries for the carbon-only LPJmL 3.5 version, the version with N limitation and with unlimited N supply.

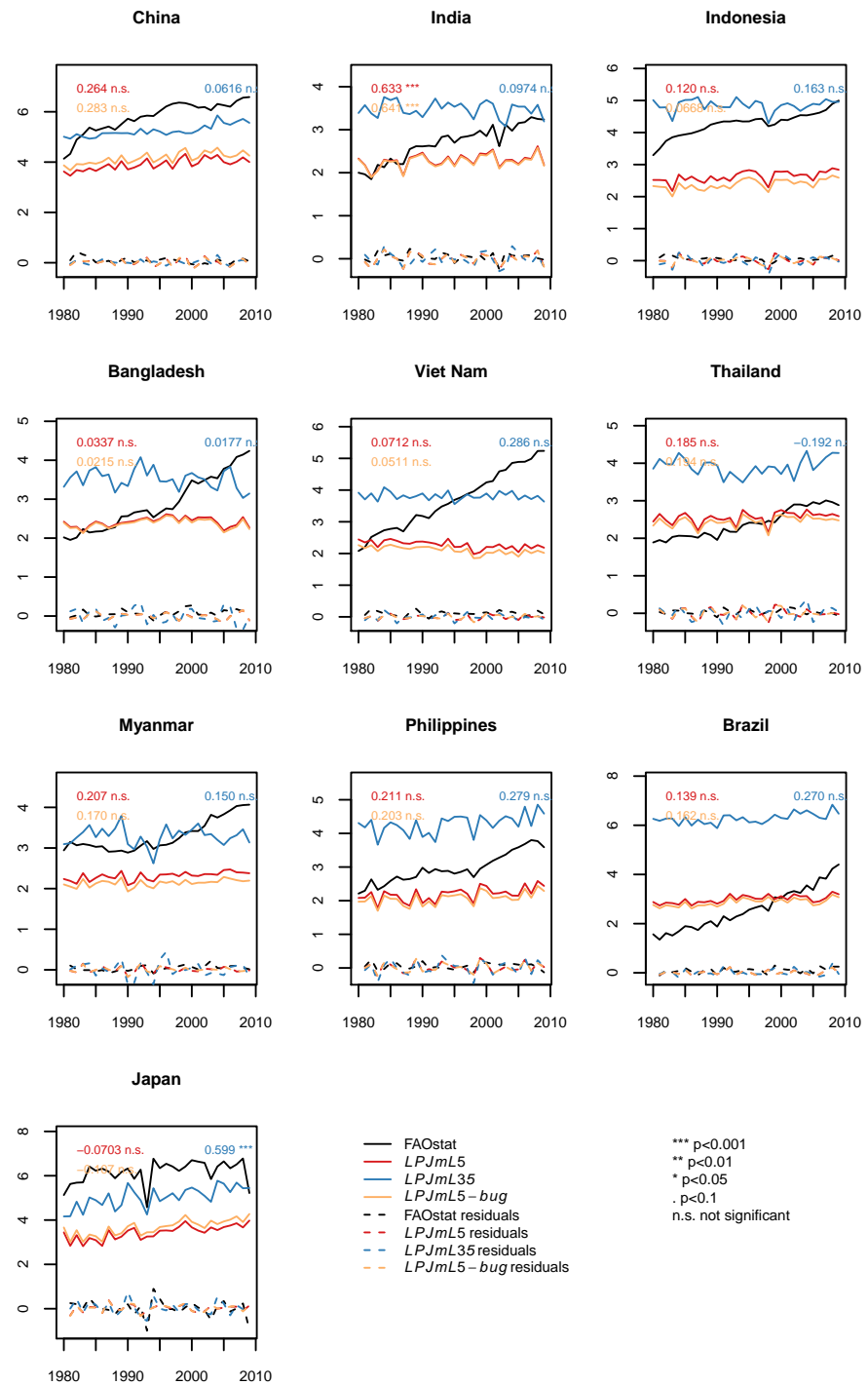


Figure S22. Rice yield simulations (in tFM ha^{-1}) for the 10 top-producing countries for the carbon-only LPJmL 3.5 version, the version with N limitation and with unlimited N supply.

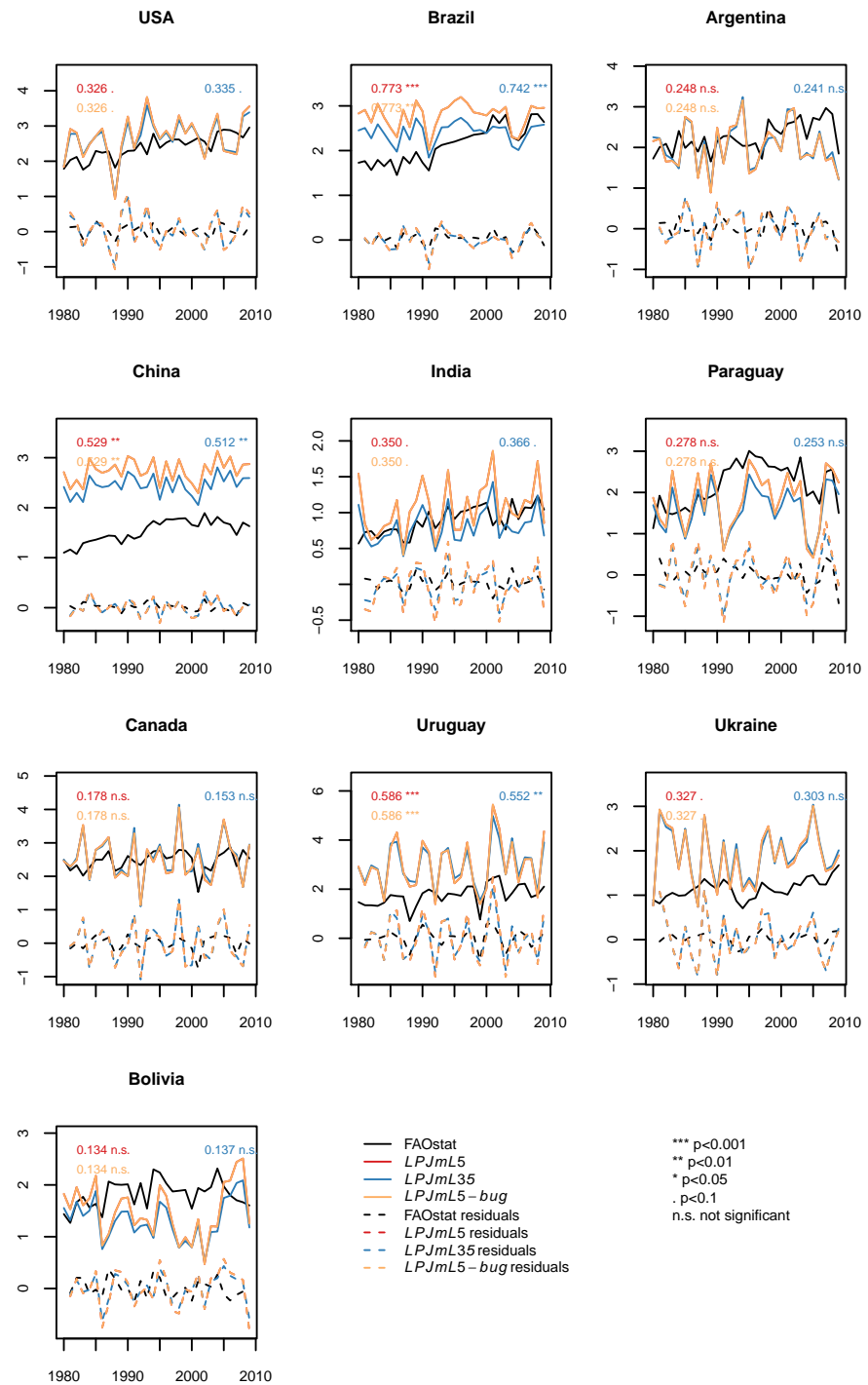


Figure S23. Soybean yield simulations (in tFM ha⁻¹) for the 10 top-producing countries for the carbon-only LPJmL 3.5 version, the version with N limitation and with unlimited N supply.